

# Artificial Intelligent Maximum Power Point Controller based Hybrid Photovoltaic/Battery System

Original Scientific Paper

**Aymen Kadhim Mohaisen**

Southern Technical University, Amara Technical Institute, Department of Electrical Power  
Amara, Iraq  
aymenks@stu.edu.iq

**Abstract** – Photovoltaic (PV) cells have non-linear properties influenced by environmental factors, including irradiation and temperature. As a result, a method known as maximum power point tracking (MPPT) was implemented to boost the PV cells' efficiency and make the most of the energy they could provide. The traditional perturb and observe (P&O) approach for determining the maximum power point tracking (MPPT) has various drawbacks, including poor steady-state performance, increased oscillation around the MPP point, and delayed reaction. As a result, this work aims to present a hybrid fuzzy logic (FL) and P&O MPPT approach to improve the PV system's performance coupled to the lithium battery storage system. Matlab/Simulink is used to bring the suggested technique to life, after which its efficacy is evaluated in the context of rapid changes in the irradiance level. According to the findings of the simulations, the suggested strategy has the potential to enhance the steady-state performance of PV systems in terms of oscillation and time response. Finally, the proposed results are compared with that obtained by the conventional P&O technique, and the stress of PV power is limited to  $\Delta P=1\text{ kW}$  and the overshoot power is limited to 5%.

**Keywords:** Artificial Intelligent Maximum Power Point Controller, photovoltaic/ battery system, fuzzy P&O controller, power management, hybrid power system

## 1. INTRODUCTION

Photovoltaic (PV) cells, also known as solar cells, have several non-linear characteristics that can impact their performance and behavior. These include the Current-Voltage (I-V) Curve, which describes the relationship between current and voltage across the cell, which is non-linear and typically follows a characteristic shape. The I-V curve consists of four regions: open circuit, short circuit, maximum power point, and reverse bias. The non-linearity arises from factors like recombination, series and shunt resistances, and temperature effects [1, 2]. Temperature dependence is another non-linear characteristic of PV cells, as temperature influences performance. As temperature increases, the output voltage decreases while the current increases, decreasing overall power output. The temperature coefficient of a PV cell quantifies this non-linear relationship.

Non-uniform illumination, such as shading or partial coverage, can significantly reduce a cell's overall power

output due to bypass diodes and current mismatch. The diode junction exhibits non-linear behavior, acting like a diode but not perfectly ideal due to non-zero idealist factors and series resistance [2]. These effects can introduce non-linear behavior in response to high-frequency light intensity or voltage variations.

Hysteresis is the phenomenon where the I-V curve of a PV cell depends on the history of the previous operation, which can be observed during rapid changes in light intensity or dynamic operating conditions. This implies that the same voltage may generate distinct currents depending on whether the voltage is rising, falling, or staying the same. Understanding and modeling these non-linear characteristics is crucial for accurately predicting and optimizing PV system performance, designing efficient power converters, maximum power point tracking (MPPT) algorithms, and overall system integration [3]. The classification of the MPPT methods can be shown in Fig.1.

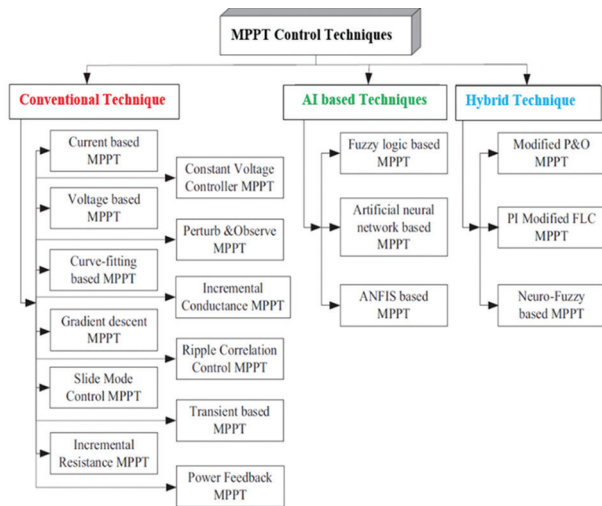


**Fig.1.** Classification of the most used MPPT techniques

The authors of [4] suggested using a constant voltage controller, sometimes known as a CVC, to maximize the peak power output of PV panels. This technique required little in the way of resources and was easy to put into practice experimentally; nevertheless, the results were less accurate and productive. Despite this, several researchers have suggested and evaluated techniques that are straightforward and inexpensive, such as the perturb and observe (P&O) and incremental conductance (IC) techniques [5-8]. Even though these methods were uncomplicated and straightforward to put into practice, they had a great deal of drawbacks.

When using a P&O approach, there is a greater amount of oscillation around the MPPT, which increases power loss and a drop in the control efficiency. In addition, the IC technique has several limitations, the most notable of which are oscillation and transitory response in the face of rapid change in solar irradiance [9]. Because of this, the variable size incremental conductance approach has been proposed as a solution to the problems currently facing the CVC, P&O, and IC procedures [9, 10].

In addition, the authors in [11, 12] offered the AI approaches based on MPPT to overcome the major difficulties in classical techniques such as fuzzy logic (FL) and neural networks (ANN). These methods based on nonlinear theory also contribute to the increased number of benefits they present compared to more traditional approaches. Consequently, they regarded a robust MPPT and had higher performance in calculating the PV module's operational point under various atmosphere conditions [13, 14]. A hybrid MPPT approach is also used to augment AI techniques such as proportional-integral (PI) with FL or ANN. This technique is used to improve AI techniques by increasing convergence speed.

A fuzzy logic-based MPPT approach was presented by Yaqoob et al. [15] to increase the dynamic response of a PV module connected to pure DC load and sub-

jected to a rapid shift in the amount of solar irradiation. Mat lab/Simulink is used to evaluate the performance of the suggested approach and verify it. Compared to the traditional IC and P&O methods, the use of FL MPPT yields superior results in terms of output quality. Also, Fapi et al. [16] reported a real-time experiment with FL-based MPPT utilizing a digital signal processing (DSP) microcontroller. The findings demonstrate that the suggested method is less complicated, efficient, and reliable than the other common approaches.

Creating a Neuro-Fuzzy MPPT controller is the subject of the study [17]. Initially, the suggested MPPT control is constructed in a state of offline operation, which is necessary for testing various ANN designs and variables. The goal of this method is to design an efficient hybrid technique. The results of the proposed MPPT controller are excellent in obtaining the optimal voltage of the module to track the MPP with a fast time response. The authors in [18] proposed a novel coordinated MPPT method for a grid-connected PV system's inverter. Both the DC boost converter, which is responsible for MPPT of the PV plant, and the inverter, which is responsible for DC voltage set-point management, specialized reactive current injection on demand, and decreased harmonic content of AC grid currents, work together to achieve the system's control goals.

A hybrid FL-P&O-based MPPT is utilized in this article to optimize the output power of the PV system regardless of the weather conditions. The main goal of this work is to provide a variable step size for the P&O using the FL method. In addition, the suggested approach for MPPT analysis is also modeled, and simulated with the help of the MATLAB simulation program. Additionally, the performance of the FL-P&O MPPT is evaluated using a variety of solar irradiances, and these results are compared to those obtained using the more traditional P&O MPPT method.

This research is organized as follows: section 2 presents photovoltaic cell modeling. Section 3 introduces a hybrid PV/battery system. Section 4 presents the proposed MPPT controller. Section 5 indicates the results and discussion, while the conclusion of this paper is presented in section 6.

## 2. PHOTOVOLTAIC CELL MODELLING

The equivalent circuit of a PV cell, also known as a solar cell, is a simplified representation that models the cell's electrical behavior [17]. It consists of several components, including the single-diode model, which includes photocurrent ( $I_{ph}$ ), diode current ( $I_d$ ), switch resistance ( $R_{sh}$ ), and series resistance ( $R_s$ ). The photocurrent ( $I_{ph}$ ) is proportional to the intensity of incident light, while the diode current ( $I_d$ ) is modeled by the p-n junction diode's behavior. The series resistance ( $R_s$ ) represents resistive losses in the cell's electrical connections and materials, representing the overall resistance in series with the diode and load [19, 20].

However, the PV cell or module current can be written from the semiconductors theory as follows [21, 22].

$$I = I_{PH} - I_o \left[ \exp\left(\frac{qV}{\alpha V_t}\right) - 1 \right] - \frac{V + R_s I}{R_p} \quad (1)$$

where  $I$  is the PV current,  $V$  is the PV voltage,  $V_t (=N_s K T/q)$  is the thermal voltage (25.7 mV at 25°C) with  $N_s$  cells of module,  $T$  is the temperature in °C,  $R_p$  and  $R_s$  are the shunt and series resistances,  $I_{PH}$  is the source of photocurrent,  $I_o$  is saturation current,  $\alpha$  is the constant factor,  $q$  is the electron's charge ( $1.60217646 \times 10^{-19}$  C),  $K$  is the Boltzmann constant ( $1.3806503 \times 10^{-23}$  J/°K). Fig. 2 shows a model PV cell.

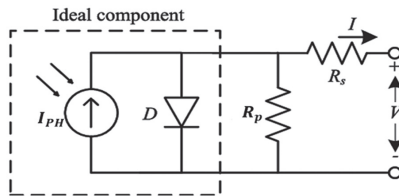


**Fig. 2.** Single-diode PV cell model

The  $I_{PH}$  can be expressed as follows [22].

$$I_{PH} = (I_{PHn} + K_i \Delta T) \frac{G}{1000} \quad (2)$$

Where the change in temperature  $\Delta T$ ,  $G$  represents the solar irradiance. To model the PV module, the diode saturation current can be determined as in (3),

$$I_o = I_{on} \left(\frac{T_n}{T}\right)^3 \exp\left[\frac{qE_g}{\alpha K} \left(\frac{1}{T_n} - \frac{1}{T}\right)\right] \quad (3)$$

Where  $I_{on}$  is the reverse saturation, temperature ( $T=25^\circ\text{C}$ ), and  $E_g$  is the band-gap energy ( $E_g=1.12$ ). moreover, this current can be written as [20,21],

$$I_{on} = \frac{I_{scn}}{\exp\left[\frac{V_{ocn}}{\alpha V_{th}}\right] - 1} \quad (4)$$

This study uses the KC200GT PV panel technology to form the required PV system. The electrical parameters under STC conditions of this panel are listed in Table 1.

**Table 1.** The electrical parameters of the KC200GT PV panel in STC conditions

Parameter	Value
$P_{mp}$	200W
$V_{oc}$	32.9 V
$V_{mp}$	26.3 V
$I_{sc}$	8.21 A
$I_{mp}$	7.61 A
$K_i$	0.0032 A/K
$K_v$	-0.123 V/K
$\alpha$	1.3
$N_s$	54

### 3. HYBRID PV/BATTERY SYSTEM

The PV-battery system is most used in PV applications, which is used in its configuration. The PV system offers the required power at the sun's availability. At the same time, the battery devices are used as a backup energy storage system at night or in partial shading effect conditions. In recent years, different control strategies have been used to control the power-sharing between the PV system and the battery [23].

Power management or power sharing control is very important to increase efficiency, and the proposed system structure is shown in this paper.

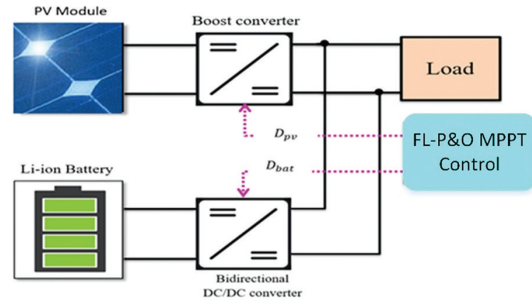


**Fig. 3.** Proposed PV/battery system structure

In Fig.3, the hybridization between the PV module and battery is considered to share the optimal power between them and the DC load side.

#### 3.1. BATTERY CONTROL MANAGEMENT

Battery management control (BMC) systems offer numerous benefits in various applications, including extended battery life, enhanced safety, optimal performance, increased efficiency, state-of-charge (SOC) monitoring, cell balancing, data logging and analysis, integration and compatibility, remote monitoring and control, scalability, and expandability. These systems help maximize battery life by monitoring and regulating charging and discharging processes, preventing overcharging, over-discharging, and overheating [24]. They also ensure safe operation by incorporating safety features like overcurrent protection, overvoltage protection, and short-circuit protection. Optimal performance is maintained by actively managing charging and discharging processes, ensuring consistent and reliable power delivery. Increased efficiency is achieved by optimizing charging algorithms, reducing power losses, and improving energy conversion efficiency. State-of-Charge (SOC) monitoring provides real-time information about remaining capacity, enabling users to accurately estimate battery runtime and plan activities accordingly. Cell balancing ensures equal charge levels in multiple cells, preventing overcharging or over-discharging [25].

In conclusion, battery management control systems are crucial for optimizing battery performance, extending battery life, ensuring safety, and improving energy

efficiency in various applications. The hybrid PV/battery system used in this paper depends on the lithium-battery model that is presented in Matlab/Simulink, as shown in Fig.4. The output voltage of the battery  $V_{btt}$  can be expressed as [25].

$$V_{btt} = E_0 - K \frac{Q}{Q - i_t} - R_b i + A_b e^{(-B i_t)} K \frac{Q}{Q - i_t} i^* \quad (5)$$

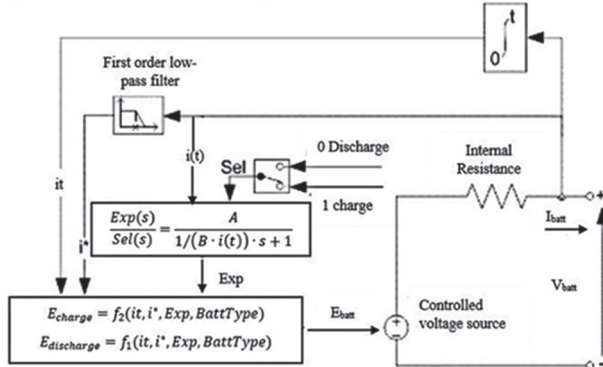


**Fig. 4.** The Battery electrical circuit module

Where  $E_0$  is the battery constant voltage (V),  $K$  is the constant of the polarization (V/Ah),  $Q$  is the capacity of the battery (Ah),  $i_t$  is the actual charge of the battery (Ah),  $R_b$  is the battery internal resistance ( $\Omega$ ),  $A_b$  is the exponential zone amplitude (V),  $B$  is the time constant inverse of the exponential zone ( $Ah^{-1}$ ),  $i^*$  is the filtered battery current (A). Also, the polarization resistance,  $Pol_{res}$  can be written as in Eq. (6), where it presents in the battery charging mode.

$$Pol_{res} = K \frac{Q}{i_t - 0.1Q} \quad (6)$$

In this paper, the reference power of the battery is controlled using a PI controller to feed the optimum duty cycle value for the DC-DC bidirectional converter, as seen in Fig. 5. The DC bus voltage is stabilized to achieve optimal performance under different loads and weather conditions. The PWM frequency of this converter is 5kHz. the indicator ( $L_{bat}$ ) 20 mH, input capacitor ( $C_1$ ) 220  $\mu$ F and output capacitor ( $C_2$ ) 470  $\mu$ F.

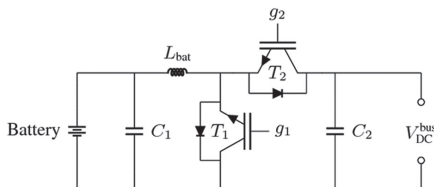


**Fig. 5.** Battery energy storage with DC/DC bidirectional converter

### 3.2. MODELLING OF BOOST CONVERTER

DC/DC boost converters offer several advantages in various applications, including voltage boost, efficient power conversion, compact size, regulated output, versatility, power source flexibility, ripple reduction, and control and protection features. These converters en-

able step-up voltages, high efficiency, compact size, and regulated output, making them ideal for low input voltage systems like battery-powered devices [26, 27]

They are also compact and lightweight, making them suitable for space constraints and integrating into various devices. Regulatory output ensures a stable power supply, especially in sensitive electronic circuits. Boost converters can operate with various power sources, such as batteries, solar panels, or fuel cells, ensuring efficient power management in renewable energy systems and electric vehicles. The circuit consists of an input inductor, a single diode, a semiconductor switch like MOSFET or IGBT, and input and output capacitors [23, 27]. The switching frequency of this converter is 20 kHz.

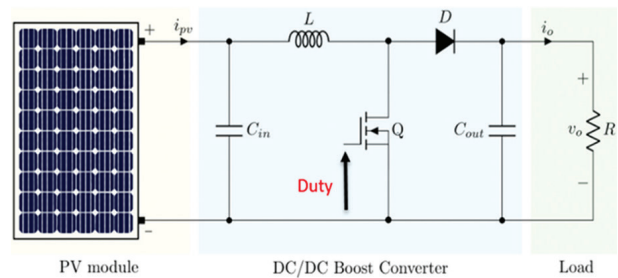


**Fig. 6.** Boost converter circuit used in MPPT controller

Managing the duty cycle  $D$  while the PWM generator executes is how the switch on the boost should be managed so that the MPPT algorithm can be implemented via the boost converter. Because of this, if the switch is in the ON state, the current travels via the inductor and the switch. After that, the energy is stored in the inductor. In contrast, when the PWM signal is withdrawn from the switch, the switch will function in an OFF state. After that, the electrical power stored via the inductor will be supplied to the output.

Furthermore, the continuous conduction mode (CCM) is mostly used in designing and finding the entire parameters of the boost circuit. Because of its low peak current, low switching device conduction losses, low turn-off losses, and high-frequency ripple amplitude, continuous conduction mode is chosen over critical conduction mode and discontinuous conduction mode in boost converters. Therefore, the theoretical equations of the boost converter can be obtained based on this mode [27]. The output voltage ( $v_o$ ) from the boost converter can be expressed as follows [27]

$$v_o = \frac{1}{1 - D} v_{pv} \quad (7)$$

Based on the above equation, the output current can be written as [26]

$$i_o = i_{pv} (1 - D) \quad (8)$$

To determine the parameters of the boost converter at CCM mode, Eq. 9 should be utilized to calculate the inductor value ( $L$ ) as [27],



$$L = \frac{v_{pv} D}{f_s \Delta i_{pv}} \quad (9)$$

where  $f_s$  is the switching frequency and  $\Delta i_{pv} = 0.3$ . In addition, the output capacitance  $C_{out}$  can be calculated as

$$C_{out} = \frac{i_o D}{f_s \Delta v_o} \quad (10)$$

where  $\Delta v_o = 0.02 v_o$ . The input capacitor  $C_{in}$  size can be determined from (11) [26, 27]:

$$C_{in} \geq \frac{D}{8 \times f_s^2 \times L \times 0.01} \quad (11)$$

#### 4. PROPOSED MPPT CONTROLLER

An adaptive fuzzy P&O MPPT approach is utilized in this work to extract the best amount of energy from the PV panel under various irradiance changes. The proposed technique mixes both advantages of the fuzzy logic and the P&O method to solve the problem oscillation that occurred with using P&O alone and increase the time response for gating maximum power under fast solar irradiance. The block diagram of the proposed system is shown in Fig. 7. This figure includes the PV system, proposed MPPT method, boost converter circuit, and the Li-ion battery module.

Fig.8 shows the block of the FL MPPT used in this research. As observed, the change in the power  $\Delta P_{pv}$  and the change in the voltage  $\Delta V_{pv}$  are represented as the inputs of the presented FL-MPPT while the duty ratio ( $D$ ) represents the output.

The membership functions for the output and inputs are done based on a triangular shape with five linguistic variables: negative big (NB), negative small (NS), zero (ZE), positive small (PS), and positive big (PB). As a result, the FL has 25 different rules.

In addition, the center of gravity method is used in this work as the defuzzification method based on the following equation.

$$Y_{COG} = \frac{\sum_{i=1}^n Y_i(X_i)X_i}{\sum_{i=1}^n Y_i(X_i)} \quad (12)$$

Where  $Y_{COG}$  is the output,  $Y_i$  is the inference result of rule  $i$ ,  $X_i$  is the output's corresponding rule  $i$ .

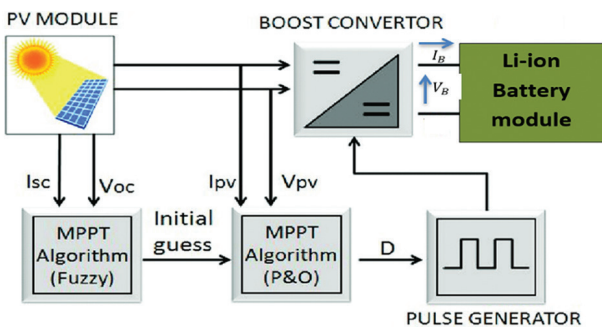


Fig. 7. The Proposed entire system

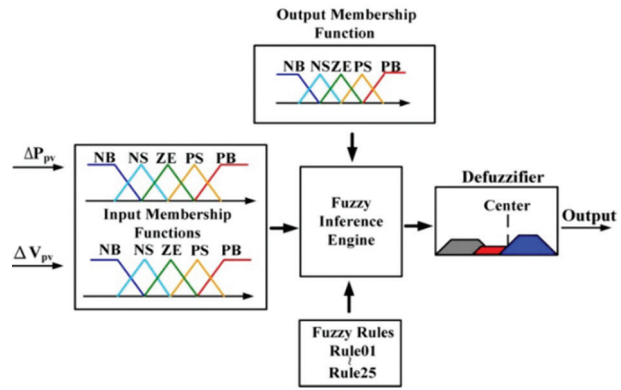


Fig. 8. Block diagram of the proposed FL MPPT controller

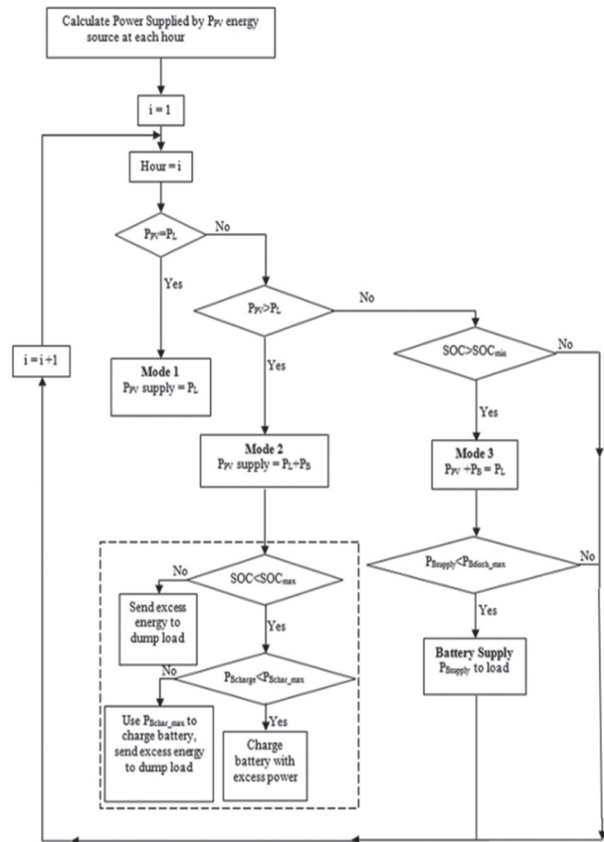


Fig. 9. Flowchart of the power management used in this study

The flowchart of the power management control is presented in Fig. 9. In this algorithm, the charge/discharge of the Li-ion battery is controlled and then the optimal duty cycle for the bidirectional is obtained. When the optimum power of the PV system is achieved, and the PV power is equal to the load power, the PV system will supply the DC demand load at the corresponding solar irradiance. The PV system will supply both the battery and load at the case of  $P_{pv} > P_L$ , and the system will operate with mode 2, and the battery will charge mode if its SOC is less than the required value. In mode 3, when  $P_{pv} + P_b = P_L$ , all generated power from the battery and PV system will convert to the load to cover the increase in the demand side.

## 5. RESULTS AND DISCUSSION

To validate the proposed method in simulation, Mat lab/Simulink 2019b has been used in this work. The PV system with a rated power of 20KW is used based on the KC200GT PV panel technology with electrical parameters, as observed in Table 1.

Based on the different 25 rule base used for the design of the proposed FL controller, the rule viewer for these rules are shown in Fig. 10. Also, the quiver plot of power and voltage of the fuzzy logic controller is seen in Fig. 11 It clear the relationship between the inputs of power and voltage for the proposed FL controller used to generate the optimal duty cycle for the boost converter.

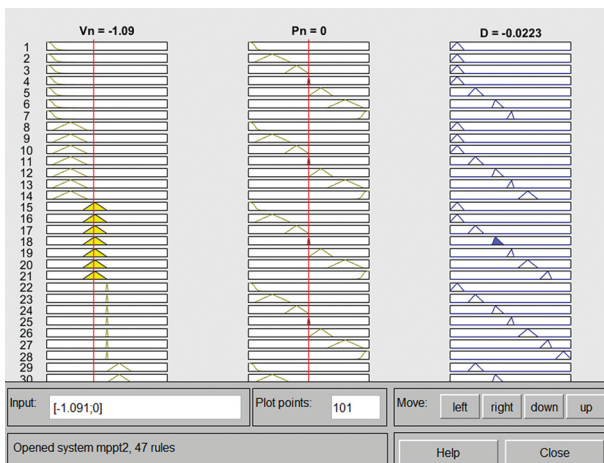


**Fig. 10.** Rule viewer of the proposed fuzzy logic controller

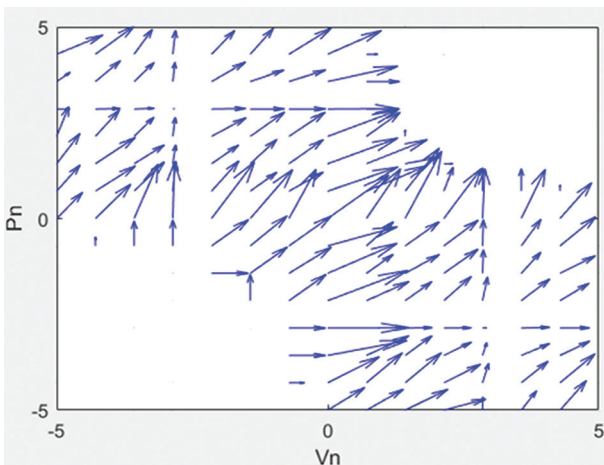


**Fig. 11.** Quiver plot of power and voltage using fuzzy logic

Furthermore, the proposed method is tested under a fast irradiance level to show the performance and compare it with the conventional technique (P&O) results. Fig. 12 shows the PV power with theoretical maximum power using the conventional P&O technique. The simulation is done for 9 seconds, and the solar irradiance is changed step by step from 250 W/m<sup>2</sup>, 500 W/m<sup>2</sup>, and 1000 W/m<sup>2</sup>. The irradiance is set to 250 W/m<sup>2</sup> from  $t=0$  to 3 sec.

In this case, the conventional P&O is responded to during response time  $t=0.8$  sec. So, the conventional P&O takes more time to reach the MPP. When the irradiance is changed from 250 to 500 W/m<sup>2</sup> at time  $t=3$  sec, the conventional P&O is reached to the MPP with a fast response but the oscillation across this point is large, ( $\Delta P=2.5$  kW) and these issues are repeated during the high irradiance level and cause more power losses. On the other hand, the proposed FL-P&O shows good results regarding fast response and oscillation. As seen in Fig. 13, the proposed method is tested under fast irradiance levels for the same case as the conventional method. As observed, the proposed method is faster than the P&O regarding response, which is reached to MPP at time  $t=0.1$ sec at lower level irradiance. The proposed method presents low oscillation issues across the high-level irradiance, where the maximum overshoot ( $\Delta P=1$  kW) leads to minimizing the power loss in the electrical system.

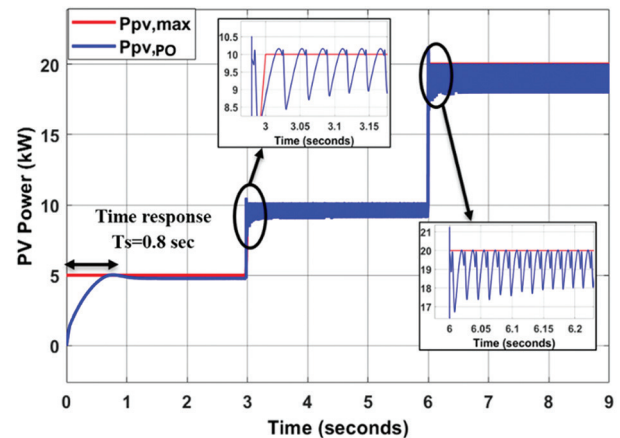


**Fig.12.** PV Power with theoretical value using the conventional P&O method

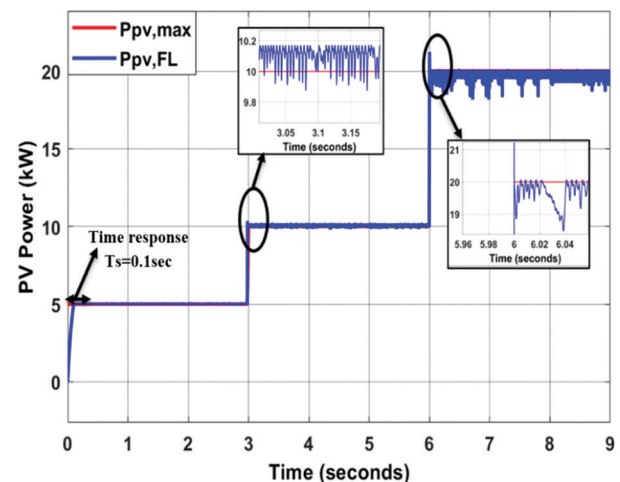


**Fig.13.** PV Power with theoretical value using the proposed FL-P&O method

Fig. 14 presents the simulation results of the PV system, including PV voltage, current, and power in the case of different irradiance levels for conventional and proposed MPPTs.

As seen, Fig. 14 a) and b) show the PV voltage and current results of FL-P&O MPPT, where voltage is little affected by the change in the irradiance, and this is because the open circuit voltage of the PV system depends strongly on the change in the temperature, not irradiance according to its mathematical equation which has a negative sign coefficient for the temperature term. The PV current is proportional to the irradiance value entered in its equation, as seen in section 2. In the conventional method (Fig. 14 c) and d)), the high ripple in the PV voltage occurs while this ripple is canceled by the proposed method, which means that robust control is achieved using the FL-MPPT. Also, when the solar irradiance is increased from 250 to 500 and then to 1000 W/m<sup>2</sup>, the proposed methods reach the maximum PV current with fast response and low harmonic oscillation in the current.

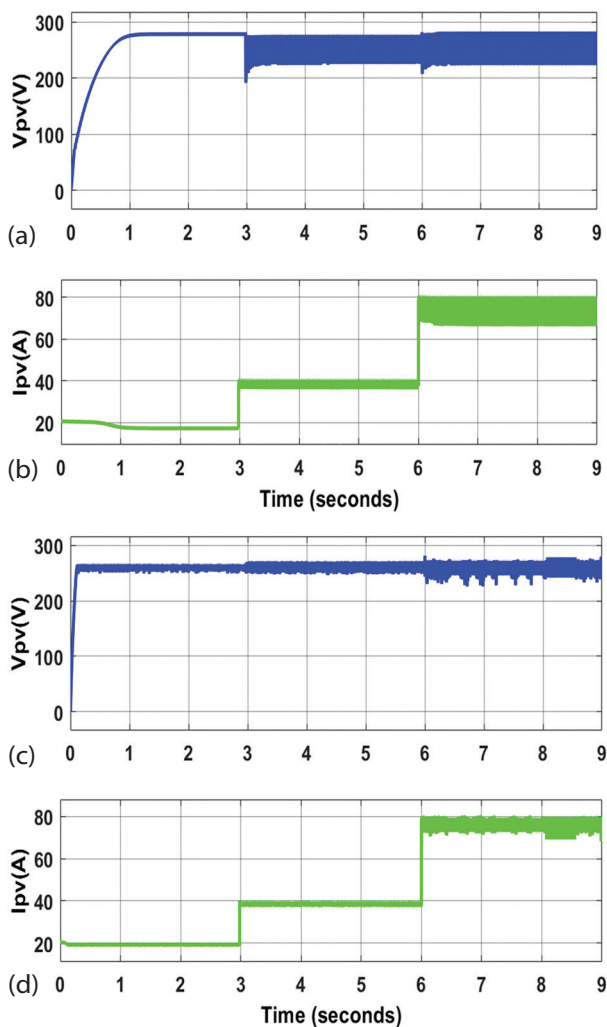


**Fig.14.** (a) PV Voltage at P&O (b) PV Current at P&O (c) PV Voltage at the proposed FL-P&O technique and (d) PV Current at the proposed FL-P&O technique

Fig. 15. shows the simulation results of the battery during a fast change in irradiance level. The SOC, voltage, and current are shown when the battery works with charging mode from the initial SOC of 50%.

At a low irradiance level, the power management system makes the proposed system work in mode 3 ( $P_{PV} + P_B = P_L$ ) where the output PV power is low and cannot cover all DC load. As a result, to supply the required demand power, both the battery and PV are operated. As seen, the battery is operated in discharge mode from  $t=0$  to  $t=3$  sec, and when the irradiance becomes high (500 and 1000 W/m<sup>2</sup>), the SOC of the battery is increased, and then the battery becomes in the charging mode, and the power management system switches the system to work with mode 2 ( $P_{PV} = P_B + P_L$ ).

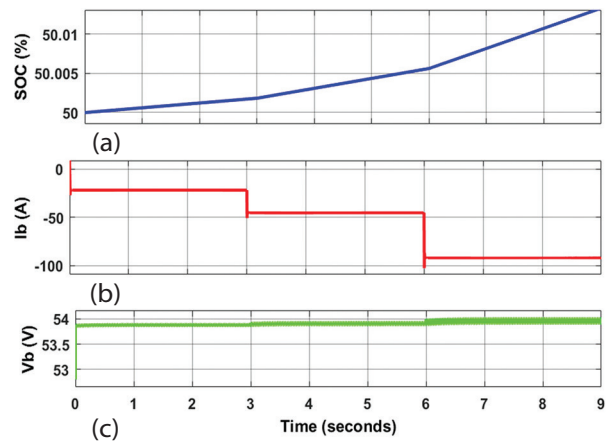


**Fig.15.** (a) The SOC of the battery, (b) the battery's current, and (c) the voltage's battery

To clear the novelty of the presented study, table 2 was added to show the comparison between the proposed method and the classical P&O in terms of the extracted power from the PV system, tracking time or time response, and the oscillation in the power. This table shows that the presented study has excellent performance under different irradiance values. As observed, the suggested method presents a high dynamic response, less oscillation, and high extracted power.

**Table 2.** Comparison between the proposed method and conventional P&O

Irradiance (W/m <sup>2</sup> )	Method	Extracted power (kW)	Time response (sec)	Oscillation (W)
200	P&O	3.7	0.99	3400
	FL-P&O	4.2	0.2	1700
400	P&O	8.7	0.87	2800
	FL-P&O	9.5	0.12	1300
600	P&O	11	0.94	3000
	FL-P&O	12	0.12	1210
800	P&O	15	0.9	2600
	FL-P&O	17	0.13	1100
1000	P&O	18	0.84	2500
	FL-P&O	20	0.11	1000

## 6. CONCLUSION

This study presents the hybrid fuzzy logic-perturb and observes (FL-P&O) maximum power point tracker (MPPT) for hybrid photovoltaic/battery systems. In

the beginning, the mathematical analysis for the model of the PV cell, the Li-ion battery, and the DC/DC boost converter are investigated. Second, the FL-P&O MPPT approach that has been presented is intended to optimize the output power of the PV system even when the irradiance is subject to rapid change. The suggested FL is modeled in Mat lab/Simulink using five distinct language variables, including ones for the derivative power (P), derivative voltage (V), and duty ratio (D). Additionally, the membership functions (MFs) for the output and inputs are carried out based on a triangle form, and the approach that is used for defuzzification is the center of gravity method. To validate the performance of the suggested technique, it is evaluated under various irradiance conditions. According to the findings of the simulations, the suggested technique performs much better than the traditional P&O method in terms of oscillation, power loss, and time response. The PV system robustness is improved, and the overshoot power is limited to 5% for irradiancies step by 250 W/m<sup>2</sup>.

## 7. REFERENCES

- [1] S. J. Yaqoob, S. Ferahtia, A. A. Obed, A. H. Rezk, N.T. Alwan, M. H. Zawbaa, S. Kamel, "Efficient Flatness Based Energy Management Strategy for Hybrid Supercapacitor/Lithium-ion Battery Power System", *IEEE Access*, Vol. 10, No. 6, 2022, pp. 132153-132163.
- [2] S. R. Sinsel, R. L. Riemke, V. H. Hoffmann, "Challenges and solution technologies for the integration of variable renewable energy sources—a review", *Renewable energy*, Vol. 145, 2019, pp. 2271-2285.
- [3] R. Bisht, A. Sikander, "An improved method based on fuzzy logic with beta parameter for PV MPPT system", *Optik*, Vol. 259, 2022, p. 168939.
- [4] D. Baimel, S. Taguchi, Y. Levron, J. Belikov, "Improved fractional open circuit voltage MPPT methods for PV systems", *Electronics*, Vol. 8, No. 3, 2019, p. 1-20.
- [5] S. J. Yaqoob, A. R. Hussein, A. L. Saleh, "Low Cost and Simple P&O-MPP Tracker Using Flyback Converter", *Solid State Technology*, Vol. 63, No. 6, 2020, pp. 9676-9689.
- [6] X. D. Liu, "Photovoltaic MPPT Control Strategy Based on Improved Conductance Increment Method", In *Journal of Physics: Conference Series*, IOP Publishing Vol. 2527, No. 1, 2023, p. 012040.
- [7] S. Motahhi, A. El Ghzizal, S. Sebti, A. Derouich, "Modeling of a photovoltaic system with modified incremental conductance algorithm for fast changes of irradiance", *International Journal of Photoenergy*, Vol. 2018, 2018, pp. 1-13.
- [8] A. L. Saleh, A. A. Obed, Z. A. Hassoun, S. J. Yaqoob, "Modeling and Simulation of A Low-Cost Perturb& Observe and Incremental Conductance MPPT Techniques In Proteus Software Based on Flyback Converter", *IOP Conference Series: Materials Science and Engineering*, Vol. 881, 2020.
- [9] L. Shang, H. Guo, W. Zhu, "An improved MPPT control strategy based on incremental conductance algorithm", *Protection and Control of Modern Power Systems*, Vol. 5, No. 1, 2020, pp. 1-8.
- [10] H. A. Sher, A. F. Murtaza, A. Noman, K. E. Ad-doweesh, K. Al-Haddad, M. Chiaberge, "A new sensorless hybrid MPPT algorithm based on fractional short-circuit current measurement and P&O MPPT", *IEEE Transactions on Sustainable Energy*, Vol. 6, No. 4, 2015, pp. 1426-1434.
- [11] M. Kermadi, E. Berkouk, "Artificial intelligence-based maximum power point tracking controllers for Photovoltaic systems: Comparative study", *Renewable and Sustainable Energy Reviews*, Vol. 69, 2017, pp. 369-386.
- [12] C. L. Liu, J. H. Chen, Y. H. Liu, Z. Z. Yang, "An asymmetrical fuzzy-logic-control-based MPPT algorithm for photovoltaic systems", *Energies*, Vol. 7, No. 4, 2014, pp. 2177-2193.
- [13] R. Bisht, A. Sikander, "A novel hybrid architecture for MPPT of PV array under partial shading conditions", *Soft Computing*, 2023, pp. 1-15.
- [14] R. Bisht, N. Kumar, A. Sikander, "Fuzzy Logic Based Improved Control Design Strategy for MPPT of Solar PV Systems", *Soft Computing: Theories and Applications: Proceedings of SoCTA 2019*, Vol. 1154, 2020, pp. 1093-1106.
- [15] S. J. Yaqoob, K. W. Nasser, Z. A. Hassoun, "Improved dynamic performance of photovoltaic panel using fuzzy logic-MPPT algorithm", *Indonesian Journal of Electrical Engineering and Computer Science*, Vol. 21, No. 2, 2021, pp. 617-624.
- [16] C. B. N. Fapi, P. Wira, M. Kamta, B. Colicchio, "Design and hardware realization of an asymmetrical fuzzy logic-based MPPT control for photovoltaic



- applications", Proceedings of the 47th Annual Conference of the IEEE Industrial Electronics Society, Toronto, Canada, 13-16 October 2021, pp. 1-6.
- [17] A. Harrag, S. Messalti, "IC-based variable step size neuro-fuzzy MPPT improving PV system performances", *Energy Procedia*, Vol. 157, 2019, pp. 362-74.
- [18] M. H. Larrode, A. A. B. Rújula, "A coordinated control hybrid MPPT algorithm for a grid-tied PV system considering a VDCIQ control structure", *Electric Power Systems Research*, Vol. 221, 2023, p. 109426.
- [19] F. A. Abbas, A. A. Obed, S. J. Yaqoob, "A comparative study between the most used MPPT methods and particle swarm optimization method for a standalone PV system under a fast change in irradiance level", *AIP Conference Proceedings*, Vol. 2804, No. 1, 2023.
- [20] S. J. Yaqoob, A. L. Saleh, S. Motahhir, E. B. Agyekum, A. Nayyar, B. Qureshi, "Comparative study with practical validation of photovoltaic monocrystalline module for single and double diode models", *Scientific Reports*, Vol. 11, No. 1, 2021, pp. 1-14.
- [21] L. P. N. Jyothy, M. R. Sindhu, "An artificial neural network based MPPT algorithm for solar PV system", Proceedings of the 4th International Conference on Electrical Energy Systems, Chennai, India, 7-9 February 2018, pp. 375-380.
- [22] L. Wang, Z. Wang, H. Liang, C. Huang, "Parameter estimation of photovoltaic cell model with Rao-1 algorithm", *Optik*, Vol. 210, 2020, p. 163846.
- [23] S. Ferahtia, A. Djeroui, T. Mesbahi, A. Houari, S. Zeghlache, H. Rezk, T. Paul, "Optimal Adaptive Gain LQR-Based Energy Management Strategy for Battery-Supercapacitor Hybrid Power System", *Energies*, Vol. 14, No. 6, 2021 pp. 1-16.
- [24] Y. Wang, Z. Sun, Z. Chen, "Development of energy management system based on a rule-based power distribution strategy for hybrid power sources", *Energy*, Vol. 175, 2019, pp. 1055-1066.
- [25] S. Ferahtia, A. Djerioui, S. Zeghlache, A. Houari, "A hybrid power system based on fuel cell, photovoltaic source and supercapacitor", *SN Applied Sciences*, Vol. 2, No. 5, 2020, pp. 1-11.
- [26] T. A. Chandel, M. Y. Yasin, M. A. Mallick, "Modeling and simulation of photovoltaic cell using single diode solar cell and double diode solar cell model", *International Journal of Innovative Technology and Exploring Engineering*, Vol. 8, No. 10, 2019.
- [27] W. Jiang, Y. F. Zhou, J. N. Chen, "Modeling and simulation of a boost converter in CCM and DCM", Proceedings of the 2nd International Conference on Power Electronics and Intelligent Transportation System, Shenzhen, China, 19-20 December 2009, pp. 288-291.